

Deep autoregressive models for the efficient variational simulation of many-body quantum systems

Or Sharir,^{*} Yoav Levine,[†] Noam Wies,[‡] and Amnon Shashua[§]
The Hebrew University of Jerusalem, 9190401, Israel

Giuseppe Carleo[¶]

Center for Computational Quantum Physics, Flatiron Institute, 162 5th Avenue, New York, NY 10010, USA

Artificial Neural Networks were recently shown to be an efficient representation of highly-entangled many-body quantum states. In practical applications, neural-network states inherit numerical schemes used in Variational Monte Carlo, most notably the use of Markov-Chain Monte-Carlo (MCMC) sampling to estimate quantum expectations. The local stochastic sampling in MCMC caps the potential advantages of neural networks in two ways: (i) Its intrinsic computational cost sets stringent practical limits on the width and depth of the networks, and therefore limits their expressive capacity; (ii) Its difficulty in generating precise and uncorrelated samples can result in estimations of observables that are very far from their true value. Inspired by the state-of-the-art generative models used in machine learning, we propose a specialized Neural Network architecture that supports efficient and exact sampling, completely circumventing the need for Markov Chain sampling. We demonstrate our approach for a two-dimensional interacting spin model, showcasing the ability to obtain accurate results on larger system sizes than those currently accessible to neural-network quantum states.

Introduction.— The theoretical understanding and modeling of interacting many-body quantum matter represents an outstanding challenge since the early days of quantum mechanics. At the heart of several problems in condensed matter, chemistry, nuclear matter, and more lies the intrinsic difficulty of fully representing the many-body wave-function, in principle needed to exactly solve Schrödinger’s equation. This circumstance is known as the quantum many-body problem, and has been tackled by several schemes of increasing complexity, ranging from mean-field theory to advanced numerical many-body techniques. Among the several approaches to the quantum many-body problem, variational methods have played an important role in the understanding of collective phenomena in interacting systems. Most notably, the application of variational wave-functions encoding many-body effects was pioneered more than 50 years ago for the study of superfluidity in Helium 4 [1] with Variational Monte Carlo (VMC). Since then, several other variational approaches have been devised for many-body quantum matter. These fall into two main categories: on one hand, the VMC family, characterized by stochastic approaches often **relying** on highly-entangled wave-functions, but with a limited variational freedom; on the other hand, relatively more recently, tensor-network approaches have been put forward, based on non-stochastic variational optimization, and most chiefly on entanglement-limited variational wave-functions [2–5]. While hugely influential in the assessment of physical properties of several in-

teracting quantum systems, both families of approaches however suffer from known limitations, in turn limiting the physical systems that can be successfully studied. Remarkably, despite substantial efforts, controllable and efficient variational approaches for strongly-interacting 2D quantum systems are still lacking. In this context, phenomena that manifest themselves on relatively large scales, or questions regarding highly entangled systems, *e.g.*, those related to the dynamics of non-equilibrium high energy states in systems which do not undergo localization [6], are currently unattainable.

A third way to perform variational studies of many-body quantum systems has been recently put forward. Inspired by the mounting success in the field of machine learning, neural-network-based architectures were proposed as variational wave functions [7]. Restricted Boltzmann machines (RBM), which represent relatively veteran machine learning constructs, were shown to be capable of representing volume-law entanglement scaling in 2D [8–11]. Recently, other neural-network architectures have been explored. Most notably, convolutional neural networks (ConvNets) – leading deep learning architectures that stand at the forefront of empirical successes in various Artificial Intelligence domains – have been applied to several bosonic systems [12, 13]. This type of architectures have been recently shown to be especially suitable for the representation of highly entangled systems [14]. Specifically, they are more expressive than RBMs, enjoying a polynomial advantage in their ability to represent volume-law entanglement.

Despite the theoretical advantage of ConvNet architectures, however, early numerical studies have been limited to relatively shallow architectures, far from the very deep networks used in modern machine learning applications. This practical limitation is mostly due to two main factors. The first limiting factor is the difficulty in effi-

^{*} or.sharir@cs.huji.ac.il

[†] yoavlevine@cs.huji.ac.il

[‡] noam.wies@cs.huji.ac.il

[§] shashua@cs.huji.ac.il

[¶] gcarleo@flatironinstitute.org

ciently obtaining quantum expectation values over ConvNet states using stochastic sampling based on Markov Chain Monte Carlo (MCMC), as is it is customary in VMC applications. The second important limiting factor is the optimization bottleneck faced when dealing with a large number of parameters. However, both limitations are routinely faced when learning deep autoregressive-models, recently introduced machine-learning techniques that have enabled previously intractable applications.

In this paper, we propose a pivotal shift in the use of Neural-network Quantum States (NQS) for many-body quantum systems, that markedly sets a discontinuity with traditionally adopted VMC methods. Inspired by the latest advances in generative machine learning models, we introduce variational states for which both the sampling and the optimization issues are substantially alleviated. Our model is composed of a ConvNet that allows direct, efficient, and i.i.d. sampling from the highly entangled wave function it represents. The network architecture draws upon successful autoregressive models for representing and sampling from probability distributions. Those are widely employed in the machine learning literature [15], and have been recently used for statistical mechanics applications [16]. We generalize these autoregressive models to treat complex-valued wave-functions, obtaining highly expressive architectures parametrizing an automatically normalized many-body quantum wave function.

Neural Autoregressive Quantum States.— We consider in the following a pure quantum system, constituted by N discrete degrees of freedom $\mathbf{s} \equiv (s_1, \dots, s_N)$ (e.g. spins, occupation numbers, etc.) such that the wave-function amplitudes $\Psi(\mathbf{s})$ fully specify its state. A full representation of Ψ entails an exponential (in N) number of complex values, which quickly becomes infeasible for modest values of N . Here we follow the approach introduced in [7], and leverage the expressive power of Artificial Neural Networks (ANN) to represent Ψ , a variational representation known as NQS. More specifically, a common choice adopted so far is to represent $\log(\Psi(\mathbf{s}))$ as a feed-forward ANN, parametrized by a possibly large number of network connections. Given an arbitrary set of quantum numbers, \mathbf{s} , the output value computation of the corresponding NQS, known as its *forward pass*, can generally be described as a sequence of K matrix-vector multiplications separated by the applications of a non-linear element-wise *activation* function $\sigma : \mathbb{C} \rightarrow \mathbb{C}$. More formally, the unnormalized log amplitudes are given by

$$\log(\Psi(\mathbf{s})) = W_K \sigma(W_{K-1} \sigma(\dots \sigma(W_1 \mathbf{s}))), \quad (1)$$

where $\mathcal{W} \equiv \{W_i \in \mathbb{C}^{r_i \times r_{i-1}}\}_{i=1}^K$, $r_0 = N$, $r_K = 1$, r_1, \dots, r_{K-1} are known as the *widths* of the network, and K as the *depth*. In practice, specialized variants of eq. 1 are commonly used, e.g. early applications have focused on shallow architectures ($k = 1$) such as Restricted Boltzmann Machines, for which the activation function is typically taken to be $\sigma(z) = \log \cosh(z)$. Other, deeper, choices are often advantageous, such as convolutional

networks, in which most of the matrices are restricted to act on a subset of the quantum numbers, computing convolutions with small filters.

Given a NQS representation of a many-body quantum state, estimating physical observables $\langle \Psi | \mathcal{O} | \Psi \rangle$ of a local operator \mathcal{O} , is in general analytically intractable, but can be realized numerically through a stochastic procedure, as done in VMC. Specifically, $\langle \Psi | \mathcal{O} | \Psi \rangle = \langle \mathcal{O}^{\text{loc}} \rangle_{\mathcal{P}}$, where $\langle \dots \rangle_{\mathcal{P}}$ denote statistical expectation values over the Born probability density $\mathcal{P}(\mathbf{s}) \equiv |\Psi(\mathbf{s})|^2$, and $\mathcal{O}^{\text{loc}} \equiv \sum_{\mathbf{s}'} \langle \mathbf{s} | \mathcal{O} | \mathbf{s}' \rangle \Psi(\mathbf{s}') / \Psi(\mathbf{s})$ is the corresponding statistical estimator. In the vast majority of VMC applications, including NQS so far, a MCMC algorithm is typically used to generate samples from $\mathcal{P}(\mathbf{s})$. While MCMC is a rather flexible technique, it comes with a large computational cost, especially for deep ANNs. In that case, generating a single sample requires many forward passes over the network, effectively setting a limit on the viable width and depth of practical NQS, in turn limiting the expressive power of the representation. Additionally, though MCMC asymptotically generates samples that are correctly distributed, in practice it can be plagued by very large autocorrelation times, and lack of ergodicity, that can severely affect the quality of the samples being generated.

In light of the limitations associated with MCMC sampling, we propose here a specialized network architecture that instead supports efficient and exact sampling, allowing to fully unlock the expressive power of deep networks. Our approach is an extension of Neural Autoregressive Density Estimators (NADE) [15] to quantum applications, resulting in what we dub *Neural Autoregressive Quantum States* (NAQS). To start with, first consider the task of representing a probability distribution with NADE models. These models build on the so-called autoregressive property, which entails a decomposition of the full probability distribution as a product of conditionals, i.e. $P(s_1, \dots, s_N) = \prod_{i=1}^N p_i(s_i | s_{i-1}, \dots, s_1)$. The power of these models comes from the observation that, for every i , the conditional probabilities p_i can be individually represented as an ANN receiving as input the variables s_1, \dots, s_{i-1} and outputting a vector $\mathbf{v}_i \equiv (v_i(s^1), v_i(s^2) \dots v_i(s^M))$ representing the unnormalized probabilities for s_i to take one of the M possible discrete values s^j , conditioned on given s_1, \dots, s_{i-1} . It is crucial that each output vector \mathbf{v}_i does not depend on the value of s_i or any of the variables appearing with a larger index, s_{i+1}, \dots, s_N , for a pre-chosen ordering. To ensure that each network outputs a valid conditional distribution, it is then sufficient to take the absolute value over each entry and normalizing it according to the l_1 norm, i.e. $p_i(s_i | s_{i-1}, \dots, s_1) = |v_i(s_i)| / \sum_{s'} |v_i(s')|$.

Even though it is possible to use N separate networks for each of the N conditional probabilities, and each accepting a variable number of inputs, in practice it is more common to use a single ANN that accepts N inputs and outputs N probability vectors. In this case, the autoregressive property is enforced by masking the

inputs s_i, \dots, s_N for the i 'th output vector, i.e. ensuring that the contributions of higher-ordered spins to the output of the network vanish. PixelCNN [17] is such an architecture, and is built as a sequence of *masked* convolutional layers, whose filters are restricted to having zeros at positions “ahead”. For example, in a one dimensional system, a filter of width R , where R is odd, would be constrained to have $(w_1, \dots, w_{(R-1)/2}, 0, \dots, 0)$, and thus the i th output of each layer depends uniquely on the indices at s_1, \dots, s_{i-1} .

A chief advantage of networks with the autoregressive property, is that directly drawing samples according to $P(\mathbf{s})$ is conceptually straightforward. One can sample each s_i in sequence, according to its given conditional probability that depends just on the previously sampled (s_1, \dots, s_{i-1}) . At a first glance it might seem that this sampling procedure would require N sequential forward passes to compute each conditional probability. However, when using the PixelCNN architecture it is possible to cache most of the computations in each forward pass, exploiting the intrinsic sparseness of the network weights [18]. Thus, the complexity of sampling a full string $s_1 \dots s_N$ can be reduced to the complexity of just a single forward pass.

Our NAQS model for representing wave-function is based on the same NADE principles so-far described. Specifically, just as probability functions can be factorized into a product of conditional probabilities, we represent a normalized wave-function as a product of normalized *conditional* wave-functions, such that

$$\Psi(s_1, \dots, s_N) = \prod_{i=1}^N \psi_i(s_i | s_{i-1}, \dots, s_1), \quad (2)$$

where $\psi_i(s_i | s_{i-1}, \dots, s_1)$ are such that, for any fixed $(s_1, \dots, s_{i-1}) \in \{1, \dots, M\}^{i-1}$, they satisfy the normalization condition $\sum_{s'} |\psi_i(s' | s_{i-1}, \dots, s_1)|^2 = 1$. If this condition holds, then a strong normalization condition for the full wave-function follows (see app. A for proof):

Claim 1 *Let $\Psi : [M]^N \rightarrow \mathbb{C}$ such that $\Psi(s_1, \dots, s_N) = \prod_{i=1}^N \psi_i(s_i | s_{i-1}, \dots, s_1)$, where $\{\psi_i\}_{i=1}^N$ are normalized conditional wave-functions. Then, Ψ is normalized, i.e., $\sum_{s_1, \dots, s_N} |\Psi(s_1, \dots, s_N)|^2 = 1$.*

As in the NADE case, we represent conditional wave-function with an ANN accepting (s_1, \dots, s_{i-1}) and outputting a complex vector $\mathbf{v}_i \equiv (v_i(s^1), v_i(s^2) \dots v_i(s^M)) \in \mathbb{C}^M$ for each of the M possible values taken by the local quantum numbers s_i . To ensure that each complex output vector represents a normalized conditional wave-function, we normalize it according to the l_2 -norm, i.e., $\psi_i(s_i | s_{i-1}, \dots, s_1) = v_i(s_i) / \sqrt{\sum_{s'} |v_i(s')|^2}$. Given this parametrization, the full wave-function amplitude $\Psi(s_1 \dots s_N)$ is easily obtained, once all the vectors $\mathbf{v}_1, \dots, \mathbf{v}_N$ have been computed. As in the probabilistic

autoregressive model, we can represent the entire NAQS by a single neural network outputting N complex vectors, as illustrated in Fig. 1a.

Moreover, there is a special relationship between a NAQS and its induced Born probability, since $|\Psi(s_1, \dots, s_N)|^2 = \prod_{i=1}^N |\psi_i(s_i | s_{i-1}, \dots, s_1)|^2$, implying that $|\psi_i(s)|^2$ is a valid conditional probability. Thus, the induced Born probability of a NAQS has the exact same structure of a NADE model. Specifically, taking the squared magnitude of its output vectors, i.e., $\bar{v}_i = |\hat{v}_i|^2$, transform NAQS into a standard NADE representation of this distribution, which importantly includes its efficient and exact sampling method. In rem contrast to standard MCMC sampling employed for correlated wave-functions, NAQS allows for direct, efficient sampling with the computational complexity of a single forward pass, as depicted in Fig. 1b.

Optimization.— The NAQS representation of many-body wave functions can be used in practice for several applications. These include for example ground-state search [7], quantum-state tomography [19], dynamics [7], and quantum circuits simulation [20]. Here we more specifically focus on the task of finding the ground state of a given Hamiltonian \mathcal{H} . In this context, we denote by $\Psi_{\mathcal{W}}$ the wave-function represented by a NAQS of a fixed architecture that is parameterized by \mathcal{W} , and we wish to find \mathcal{W} values that minimize the energy, i.e.,

$$E(\mathcal{W}) \equiv \langle \Psi_{\mathcal{W}} | \mathcal{H} | \Psi_{\mathcal{W}} \rangle = \mathbb{E}_{\mathbf{s} \sim |\Psi_{\mathcal{W}}|^2} [E_{\text{loc}}(\mathbf{s}; \mathcal{W})] \quad (3)$$

$$E_{\text{loc}}(\mathbf{s}; \mathcal{W}) \equiv \sum_{s'} \mathcal{H}_{\mathbf{s}, s'} \frac{\Psi_{\mathcal{W}}(s')}{\Psi_{\mathcal{W}}(\mathbf{s})} \quad (4)$$

$$\mathcal{W}^* = \underset{\mathcal{W}}{\text{argmin}} E(\mathcal{W}), \quad (5)$$

where \mathcal{H} is usually a highly sparse matrix, and so computing E_{loc} for a given sample takes at most $O(N)$ forward passes.

The common approach for solving the optimization problem above with an NQS is to estimate the gradient of $E(\mathcal{W})$ with respect to \mathcal{W} , and use variants of gradient descent to find the minimizer of $E(\mathcal{W})$. Estimating the gradient can be done by first employing a variant of the log-derivative trick, i.e.,

$$\frac{\partial E}{\partial \mathcal{W}} = \mathbb{E}_{\mathbf{s} \sim |\Psi_{\mathcal{W}}|^2} \left[2 \text{Re} \left((E_{\text{loc}}(\mathbf{s})^* - E^*) \frac{\partial \log \Psi_{\mathcal{W}}}{\partial \mathcal{W}} \right) \right]. \quad (6)$$

Now, while we can efficiently compute the log derivative of $\Psi_{\mathcal{W}}$, exactly computing the expected value is intractable, but we can still approximate it by computing its value over a finite batch of samples $\{\mathbf{s}^{(i)}\}_{i=1}^B$:

$$\frac{\partial E}{\partial \mathcal{W}} \approx \frac{2}{B} \sum_{i=1}^B \text{Re} \left(\left(E_{\text{loc}}^*(\mathbf{s}^{(i)}) - \frac{1}{B} \sum_{j=1}^B E_{\text{loc}}^*(\mathbf{s}^{(j)}) \right) \frac{\partial \log \Psi_{\mathcal{W}}}{\partial \mathcal{W}} \right). \quad (7)$$

(a) Neural Autoregressive Quantum State

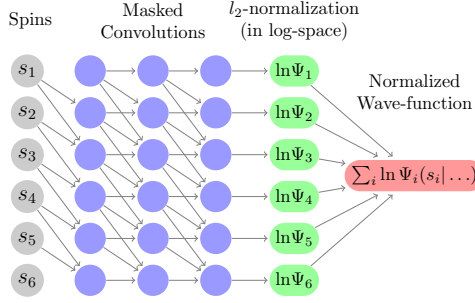
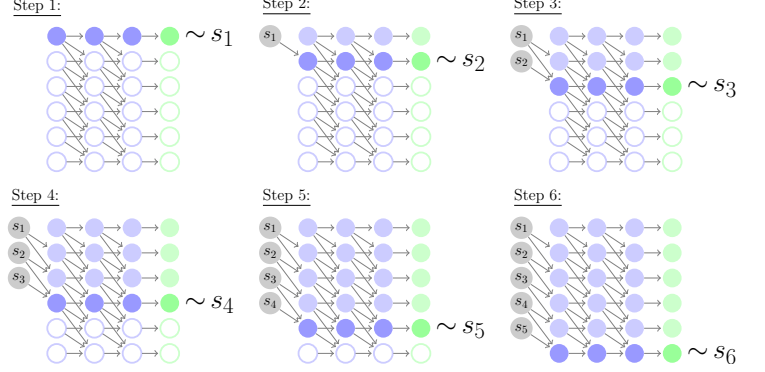
(b) Sampling $(s_1, \dots, s_6) \sim |\Psi(s_1, \dots, s_6)|^2$ 

FIG. 1. A Neural Autoregressive Quantum State is a neural network that represents a normalized wave-function, $\Psi(s_1, \dots, s_N)$, by factoring it to a sequence of normalized *conditional* wave-functions, denoted by $\Psi_i(s_i|s_{i-1}, \dots, s_1)$ for the i 'th particle (see eq. 2). The network represents these conditional wave-functions as vector outputs that depend just on previous particles, which are then normalized according to the l_2 -norm. This method is inspired by how autoregressive neural networks represent a normalized probability via the chain rule, i.e., $P(x_1, \dots, x_N) = \prod_i P(x_i|x_{i-1}, \dots, x_1)$. In practice, the network represents the conditional wave-functions in log-space for numerical stability, i.e. the conditional wave-functions are represented as $\ln \Psi_i$, the l_2 -normalization is realized by the operation $v_i - 0.5 \ln \sum_k |\exp(v_k)|^2$, and the product is replaced by a sum. (a) Illustration of a deep 1D-convolutional NAQS model following the PixelCNN [17] architecture. Each column of nodes represent a layer in the network, starting with the input layer representing the N -particle configuration (s_1, \dots, s_N) . Each internal node in the graph is a complex vector computed according to its layer type. Namely, masked convolutions are limited to having local connectivity, where a node at the j 'th row is only connected to nodes with connections to s_i where $i < j$. All inputs to a node at the l 'th layer are multiplied by a matrix $W^{(l)}$, shared across all rows in the same layer, and followed by applying a non-linear element-wise function $\sigma : \mathbb{C} \rightarrow \mathbb{C}$. (b) Depicts the exact sampling algorithm for NAQS, where empty nodes represent unused nodes, and filled but faded nodes represent cached results from previous steps. The quantum number of each particle is generated sequentially, by computing its respective conditional wave-function, and sampling according to the squared magnitude. Notice that only a single row is processed at each step, and so sampling a complete configuration has the same runtime as a single forward pass.

The quality of the above approximation depends on the batch size, B , but also on the degree of correlations between the individual samples. The advantages of our direct sampling method supported by NAQS over MCMC are twofold in this context: (i) Faster sampling: each individual sample can be generated with fewer network passes, and generating a batch of samples is embarrassingly parallel, as opposed to the sequential nature of MCMC; (ii) Faster convergence: because the generated samples are exact and i.i.d., and so result in more accurate estimates of the gradient at each step.

It is also worth remarking that NAQS allow to effectively move the scope and potentialities of variational quantum states significantly closer to the state-of-the-art in ML. This is mostly because the inherent complexity of sampling from deep networks with MCMC has limited early NQS applications to rather shallow neural-network architectures. Below, we empirically demonstrate that NAQS coupled with these advanced optimization procedure can find ground states of very large systems in a significantly shorter amount of time.

Experiments.— As a first benchmark for our approach, we consider a case where MCMC sampling can be strongly biased. A paradigmatic quantum system exhibiting this issue is found in the ferromagnetic phase of the transverse field Ising model. The Hamiltonian for

h	NAQS Energy	QMC Energy	NAQS $\langle \sigma_z \rangle$	QMC $\langle \sigma_z \rangle$
2	-2.4096022(2)	-2.40960(3)	0.78326(2)	0.78277(38)
2.5	-2.7476550(5)	-2.74760(3)	0.57572(3)	0.57566(63)
3	-3.1739005(5)	-3.17388(4)	0.16179(4)	0.16207(54)
3.5	-3.6424799(3)	-3.64243(4)	0.11094(3)	0.11011(30)
4	-4.1217979(2)	-4.12178(4)	0.09725(2)	0.09728(24)

TABLE I. Shows estimating ground states observables using NAQS is very accurate. for each h we optimize NAQS using two stages. In the first noisy stage we use small batch of 100 samples, then after the NAQS became closer to the ground state we increase the batch size to reduce the noise in the gradient. Afterward the observables estimation done with $\{x\}_{n=1}^{1200000} \sim |\psi(x)|^2$

this model is given by:

$$H = -J \sum_{\langle i,j \rangle} \sigma_z^i \sigma_z^j - \Gamma \sum_i \sigma_x^i, \quad (8)$$

where the summation runs over pairs of lattice edges. Here we study the case of a 2D square lattice with open boundary conditions, and for varying strenghts of the transverse field. The system is in a ferromagnetic phase when the transverse magnetic field Γ is weak with respect to the coupling constant, and specifically in 2D when $\Gamma < \Gamma_c \simeq 3.044J$ [21].

In order to verify the correctness of the model pro-

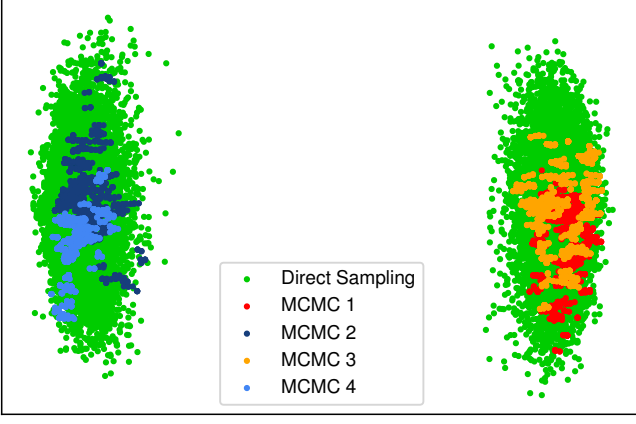


FIG. 2. The ground state of Hamiltonian 8 is a superposition of two oppositely oriented states. The i.i.d sampling enabled by our model explores the entire ground state distribution, as opposite to MCMC sampling that is stuck on a orientation it started on. The figure shows a PCA 2D visualization of generated samples. We train the NAQS on a 12×12 system with $\Gamma = 2J$, and then sample from this wave-function. We sample 20000 spin configuration directly $|\psi(x)|^2$ (Green), and additionally 8000 spin configuration sampled with 4 different Markov chains after a warm-up of 200000 sweeps.

posed in section 2, we begin by comparing the ground state energy and system magnetization obtained for a 12×12 system with those obtained by an unbiased quantum Monte Carlo (QMC) simulation. Table I shows that our model achieves very high accuracy for both magnetization and energy densities for different transverse field values across the phase diagram: when the system is in the ferromagnetic phase, the normal phase, and near the phase transition.

In order to quantify the behavior of our model in a region of broken symmetry, we consider the case of a transverse-field deep in the ferromagnetic region, namely $\Gamma = 2J$. The PCA visualization in Fig. 2 shows that for this value of Γ the MCMC chains initialized at one of the oriented states composing the ground state are stuck at that specific orientation and cannot come around to sampling spin configurations that correspond to the opposite orientation. In contrast, spin configurations sampled directly from the distribution by using our proposed technique include equally probable configurations from both orientations. The ergodicity breaking in local MCMC is also directly quantifiable by the expectation value of the total magnetization $m = \langle \sum_i \sigma_i^z \rangle$, for which we expect $m = 0$ on any finite lattice. Fig 3 (lower panel) shows that, in contrast to the MCMC case, the independent sampling enabled by our model correctly explores the two relevant ferromagnetic states (in agreement to the visualization of Fig. 2) and, after variational optimization, reaches a value close to a total zero magnetization. Additionally, as expected, the absolute value of the total magnetization is also correctly recovered by our model. Specifically, we find $\langle |\sigma_z| \rangle \simeq 0.78$, as shown in Fig 3 (up-

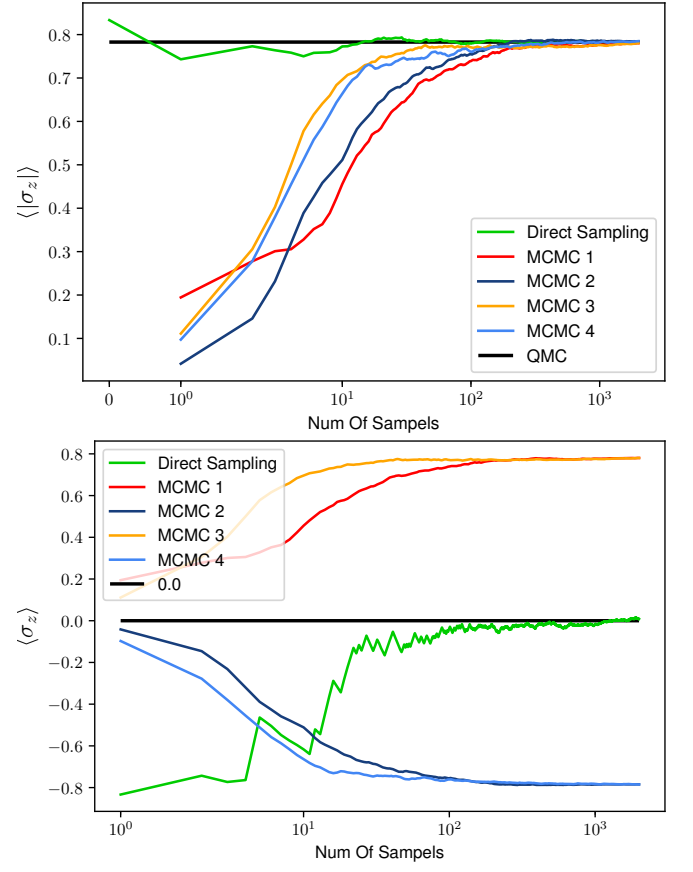


FIG. 3. The inability to produce i.i.d samples leads to incorrect magnetization estimation via the MCMC procedure. We optimize a NAQS on a 12×12 system for a transverse field Ising model with $\Gamma = 2J$, and then estimate $\langle \sigma_z \rangle$, $\langle |\sigma_z| \rangle$ using MCMC and Monte Carlo with i.i.d sampling. For the MCMC estimation we use 4 different chains and take 1 out of 100 samples to reduce correlations. The direct sampling achieves the correct value of $\langle |\sigma_z| \rangle = 0.78$ much faster than the Markov chain sampling. Moreover, it correctly achieves zero magnetization, $\langle \sigma_z \rangle = 0$, where Markov chain sampling fails altogether.

per panel).

The limitation of the MCMC procedure in providing independent samples is not only conceptually relevant, but it can also have consequences on the quality of the resulting ground-state approximations. In Fig. 4, we show the training procedure for the transverse-field $\Gamma = 3J$, close to the critical value. The same NAQS architecture was trained once with the i.i.d. sampling procedure and once with different MCMC chains. The optimization advantage obtained when relying on independent samples clearly emerges from those figures - this procedure is much quicker and results in a significantly more accurate ground state energy (upper panel) and energy variance $\langle H^2 \rangle - \langle H \rangle^2$ (lower panel).

Overall, the above presented experiments provide a demonstration for the correctness of our model, and for the power of the direct sampling procedure enabled by it.

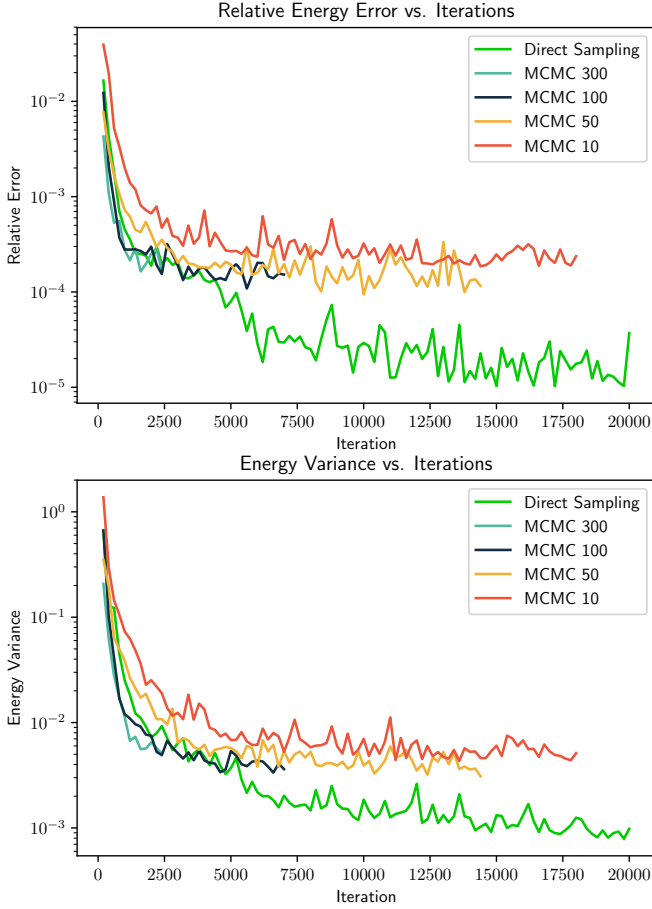


FIG. 4. Comparing the effects of the sampling method, either MCMC or direct sampling, on the training procedure for the transverse-field Ising model with $\Gamma = 3J$, close to the critical value, on a large (21×21) lattice. We use the same network architecture and optimization method in all experiments, namely, we use ADAM [?] for a maximum of 20K iterations and a batch size of 100 samples per iteration. When using MCMC, samples are taken every $k \in \{10, 50, 100, 300\}$ steps in the chain, where increasing k decreases the correlation between samples at the expense of increased computational cost. The top panel shows the relative error to the minimal energy found for this system in our experiments. The bottom panel shows the energy variance. Since MCMC takes a considerable time to complete just a single iteration, we have restricted the training to maximum of 100 hours. Notice that our direct sampling method performs as well or better than the MCMC method with $k = 300$, but can perform many more iterations at the same time. On the other hand, by using smaller k values MCMC can perform more iterations, but the increased correlation causes the optimization to get stuck at higher energy error and variance.

Discussion.— In this work, we have shown a scheme to facilitate the practical employment of contemporary deep learning architectures to the modeling of many-body quantum systems. This constitutes a striking improvement over currently used RBM methods that are limited to only hundreds of parameters, and very shallow

networks. A further practical advantage we gain is the ability to make use of the substantial body of knowledge regarding optimization of these architectures that is accumulating in the deep learning literature. We empirically demonstrate that by employing common deep learning optimization methods such as stochastic gradient descent (SGD), our direct sampling approach allows us to train very large convolutional networks (depth 20, input size 21×21 , ~ 1 million parameters), and to represent many body systems which MCMC-based techniques, following the standard VMC philosophy would not be able to optimize in any reasonable amount of time. Our presented experiments demonstrate that even for relatively simple systems MCMC sampling can fail, and the i.i.d. sampling enabled by our model succeeds. Relying on the theoretically promising results regarding convolutional networks' capabilities in representing highly entangled systems [14], we view the enabling of their optimization as an integral step in reaching currently unattainable insight on a vast variety of quantum many body phenomena.

ACKNOWLEDGMENTS

This work is supported by ISF Center grant 1790/12 and by the European Research Council (TheoryDL project). Yoav Levine is supported by the Adams Fellowship Program of the Israel Academy of Sciences and Humanities. QMC simulations for the 2D Transverse-Field Ising Model have been performed using the open-source ALPS Library [22].

Appendix A: Proof of Claim 1

The proof follows an induction argument. For $N = 1$, it holds that $\Psi(s_1) \equiv \Psi_1(s_1)$, and so Ψ is normalized because Ψ_1 is normalized with respect to s_1 . Assume the claim holds for $N = k$, then for $N = k + 1$ we first define $\tilde{\Psi}(s_1, \dots, s_k) \equiv \prod_{i=1}^k \Psi_i(s_i | s_{i-1}, \dots, s_1)$, and so

$$\begin{aligned} & \sum_{s_1, \dots, s_{k+1}} |\Psi(s_1, \dots, s_{k+1})|^2 \\ &= \sum_{s_1, \dots, s_{k+1}} \prod_{i=1}^{k+1} |\Psi_i(s_i | s_{i-1}, \dots, s_1)|^2 \\ &= \sum_{s_1, \dots, s_k} \left(\prod_{i=1}^k |\Psi_i(s_i | s_{i-1}, \dots, s_1)|^2 \right) \overbrace{\sum_{s_{k+1}} |\Psi_{k+1}(s_{k+1} | s_k, \dots, s_1)|^2}^{*=1} \\ &= \sum_{s_1, \dots, s_k} \tilde{\Psi}(s_1, \dots, s_k) \stackrel{**}{=} 1, \end{aligned}$$

where (*) is because Ψ_{k+1} is a normalized conditional wave function, and (**) because of the induction assumption. \square

- [1] W. L. McMillan, “Ground State of Liquid He4,” *Physical Review* **138**, A442–A451 (1965).

- [2] Mark Fannes, Bruno Nachtergaele, and Reinhard F. Werner, “Finitely correlated states on quantum spin chains,” *Communications in mathematical physics* **144**, 443–490 (1992).
- [3] David Perez-García, Frank Verstraete, Michael M Wolf, and J Ignacio Cirac, “Matrix product state representations,” *Quantum Information and Computation* **7**, 401–430 (2007).
- [4] Frank Verstraete and J Ignacio Cirac, “Renormalization algorithms for quantum-many body systems in two and higher dimensions,” *arXiv preprint cond-mat/0407066* (2004).
- [5] Guifré Vidal, “Class of quantum many-body states that can be efficiently simulated,” *Physical review letters* **101**, 110501 (2008).
- [6] Ehud Altman and Ronen Vosk, “Universal dynamics and renormalization in many-body-localized systems,” *Annu. Rev. Condens. Matter Phys.* **6**, 383–409 (2015).
- [7] Giuseppe Carleo and Matthias Troyer, “Solving the quantum many-body problem with artificial neural networks,” *Science* **355**, 602–606 (2017).
- [8] Dong-Ling Deng, Xiaopeng Li, and S Das Sarma, “Quantum entanglement in neural network states,” *Physical Review X* **7**, 021021 (2017).
- [9] Jing Chen, Song Cheng, Haidong Xie, Lei Wang, and Tao Xiang, “Equivalence of restricted boltzmann machines and tensor network states,” *Phys. Rev. B* **97**, 085104 (2018).
- [10] Ivan Glasser, Nicola Pancotti, Moritz August, Ivan D. Rodriguez, and J. Ignacio Cirac, “Neural-network quantum states, string-bond states, and chiral topological states,” *Phys. Rev. X* **8**, 011006 (2018).
- [11] Raphael Kaubruegger, Lorenzo Pastori, and Jan Carl Budich, “Chiral topological phases from artificial neural networks,” *Physical Review B* **97**, 195136 (2018).
- [12] Hiroki Saito and Masaya Kato, “Machine Learning Technique to Find Quantum Many-Body Ground States of Bosons on a Lattice,” *Journal of the Physical Society of Japan* **87**, 014001 (2017).
- [13] Kenny Choo, Giuseppe Carleo, Nicolas Regnault, and Titus Neupert, “Symmetries and Many-Body Excitations with Neural-Network Quantum States,” *Physical Review Letters* **121**, 167204 (2018).
- [14] Yoav Levine, Or Sharir, Nadav Cohen, and Amnon Shashua, “Quantum entanglement in deep learning architectures,” *Physical review letters* (2019).
- [15] Benigno Uribe, Marc-Alexandre Cote, Karol Gregor, Iain Murray, and Hugo Larochelle, “Neural Autoregressive Distribution Estimation,” *Journal of Machine Learning Research* () **17**, 1–37 (2016).
- [16] Dian Wu, Lei Wang, and Pan Zhang, “Solving Statistical Mechanics using Variational Autoregressive Networks,” (2018).
- [17] Aaron van den Oord, Nal Kalchbrenner, Lasse Espeholt, Oriol Vinyals, Alex Graves, *et al.*, “Conditional image generation with pixelcnn decoders,” in *Advances in Neural Information Processing Systems* (2016) pp. 4790–4798.
- [18] Prajit Ramachandran, Tom Le Paine, Pooya Khorrami, Mohammad Babaeizadeh, Shiyu Chang, Yang Zhang, Mark A Hasegawa-Johnson, Roy H Campbell, and Thomas S Huang, “Fast generation for convolutional autoregressive models,” *arXiv preprint arXiv:1704.06001* (2017).
- [19] Giacomo Torlai, Guglielmo Mazzola, Juan Carrasquilla, Matthias Troyer, Roger Melko, and Giuseppe Carleo, “Neural-network quantum state tomography,” *Nature Physics* **14**, 447 (2018).
- [20] Bjarni Jnsson, Bela Bauer, and Giuseppe Carleo, “Neural-network states for the classical simulation of quantum computing,” *arXiv:1808.05232 [cond-mat, physics:physics, physics:quant-ph]* (2018), *arXiv:1808.05232*.
- [21] Henk W. J. Blte and Youjin Deng, “Cluster Monte Carlo simulation of the transverse Ising model,” *Physical Review E* **66** (2002), 10.1103/PhysRevE.66.066110.
- [22] B. Bauer, L. D. Carr, H. G. Evertz, A. Feiguin, J. Freire, S. Fuchs, L. Gamper, J. Gukelberger, E. Gull, S. Guertler, A. Hehn, R. Igarashi, S. V. Isakov, D. Koop, P. N. Ma, P. Mates, H. Matsuo, O. Parcollet, G. Pawowski, J. D. Picon, L. Pollet, E. Santos, V. W. Scarola, U. Schollwck, C. Silva, B. Surer, S. Todo, S. Trebst, M. Troyer, M. L. Wall, P. Werner, and S. Wessel, “The ALPS project release 2.0: open source software for strongly correlated systems,” *Journal of Statistical Mechanics: Theory and Experiment* **2011**, P05001 (2011).